




Alumina-supported cobalt phosphide as a new catalyst for preferential CO oxidation at high temperatures

Siqi Wang, Yanzhao Cui, Yan Shi, Zhiwei Yao, Qingyou Liu & Yue Sun

To cite this article: Siqi Wang, Yanzhao Cui, Yan Shi, Zhiwei Yao, Qingyou Liu & Yue Sun (2019): Alumina-supported cobalt phosphide as a new catalyst for preferential CO oxidation at high temperatures, Phosphorus, Sulfur, and Silicon and the Related Elements, DOI: 10.1080/10426507.2019.1571492

To link to this article: <https://doi.org/10.1080/10426507.2019.1571492>

 View supplementary material 

 Published online: 10 Feb 2019.

 Submit your article to this journal 

 View Crossmark data 



Alumina-supported cobalt phosphide as a new catalyst for preferential CO oxidation at high temperatures

Siqi Wang^a, Yanzhao Cui^a, Yan Shi^a, Zhiwei Yao^a , Qingyou Liu^b , and Yue Sun^a

^aDepartment of Petrochemical Engineering, College of Chemistry Chemical Engineering and Environmental Engineering, Liaoning Shihua University, Fushun, P. R. China; ^bKey Laboratory of High-temperature and High-pressure Study of the Earth's Interior, Institute of Geochemistry, Chinese Academy of Sciences, Guiyang, P. R. China

ABSTRACT

Novel alumina-supported cobalt phosphide catalysts (designated as CoP-3, CoP-10, CoP-20 and CoP-40) prepared from the precursors with Co loadings of 3, 10, 20 and 40 wt% by H₂-temperature-programmed reaction were investigated as potential catalysts for preferential CO oxidation (PROX) in excess H₂ at high temperatures. It was found that the catalytic activities of these Co₂P/ γ -Al₂O₃ catalysts were related to their Co loadings. The CoP-10 catalyst showed the best PROX performance in temperature range of 220–240 °C, which was attributed to its optimal microstructures (high surface area, small particle size and big amount of active site).

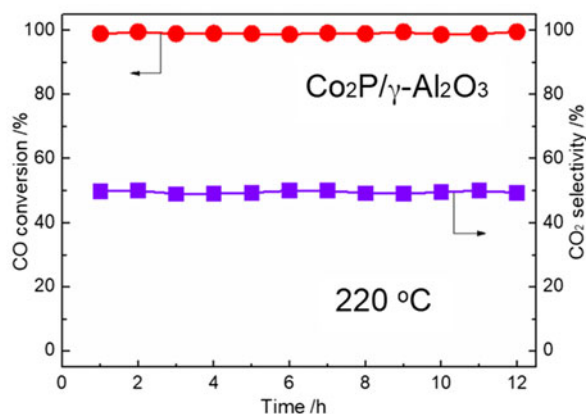
ARTICLE HISTORY

Received 22 October 2018
Accepted 15 January 2019

KEYWORDS

Alumina-supported cobalt phosphide; preferential CO oxidation; H₂-rich stream; Co loading

GRAPHICAL ABSTRACT



Introduction


Transition metal phosphides are a group of compounds with interesting chemical/physical properties and potential applications in various fields, such as electronics, magnetism, photonics, catalysis and so on.^[1–4] In particular, transition metal phosphides have been regarded as promising substitutes for noble metal catalysts, owing to their Pt-like performance as catalysts in a variety of hydrogen-involved reactions, such as hydrogenation and hydrotreating,^[5,6] N₂H₄ decomposition,^[7–9] and hydrogen evolution reactions.^[2,10,11] However, these phosphide catalysts have received far less attention in reactions involving oxygen-related species. Our previous work has shown that phosphides of Mo, W, Fe, Co and Ni exhibit good activities for NO dissociation (Fe₂P > Co₂P > MoP > WP > Ni₂P) but the phosphide

catalyst deactivation is inevitable because of surface oxidation by NO.^[12,13] Subsequently, we have found that oxygen species from NO dissociation occurred on phosphide surface can be removed efficiently by H₂ or CO, and thus the phosphide catalyst can maintain stable activity for NO dissociation in the NO/CO or NO/H₂ reaction.^[12,13]

In order to expand the field of phosphide catalysts in noble-metal catalyzed reactions involving oxygen-related species, in this study the preferential CO oxidation (PROX) in excess H₂ was selected as a probe reaction to investigate the activity of phosphide catalysts. It was well known that various catalyst systems such as Pt-Fe,^[14,15] Pt-Ni,^[16,17] Pt-Co,^[18] Cu-Ce,^[19–21] Ir-Fe,^[22] Au-Ce,^[23] and so on, with good performances have been utilized as catalysts for PROX. These catalysts were usually expected to show high activity for CO oxidation

CONTACT Qingyou Liu  liuqingyou@vip.gyig.ac.cn

Color versions of one or more of the figures in the article can be found online at www.tandfonline.com/gpss.

 Supplemental data for this article can be accessed on the publisher website.

© 2019 Taylor & Francis Group, LLC

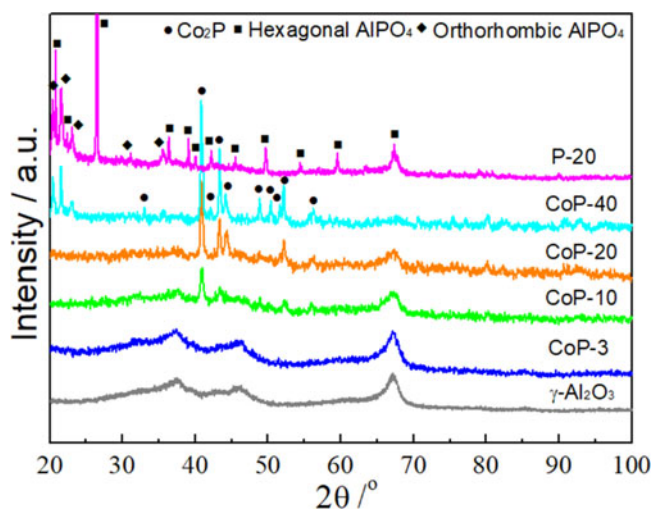


Figure 1. XRD patterns of the $\text{Co}_2\text{P}/\gamma\text{-Al}_2\text{O}_3$ catalysts with various Co loadings as well as $\text{P}/\gamma\text{-Al}_2\text{O}_3$ sample and $\gamma\text{-Al}_2\text{O}_3$ supporter for comparison.

under the typical operating temperature (ca. 80 °C) of the proton exchange membrane fuel cell. Due to the loss of heat energy for cooling H_2 -rich gas from water gas shift (WGS) reaction, operation at higher temperature, e.g., at about 210–240 °C, may be more attractive for PROX catalyst.^[24] On the other hand, the development of low-cost non-noble metal catalysts for PROX with suitable performance was of great importance and was also a meaningful challenge in industrial chemistry. In this work, we reported that the $\text{Co}_2\text{P}/\gamma\text{-Al}_2\text{O}_3$ catalysts with different Co loadings were active for PROX and they showed similar PROX activity to $\text{Pt}/\gamma\text{-Al}_2\text{O}_3$ catalyst at high temperatures. And the techniques of XRD, BET, and TEM were adopted for the characterization of the $\text{Co}_2\text{P}/\gamma\text{-Al}_2\text{O}_3$ catalysts, and to give insights into the effect of Co loading on the catalytic activity of $\text{Co}_2\text{P}/\gamma\text{-Al}_2\text{O}_3$ catalyst for preferential CO oxidation reaction.

Results and discussion

Microstructural characterization

Figure 1 shows the XRD patterns of the $\text{Co}_2\text{P}/\gamma\text{-Al}_2\text{O}_3$ catalysts with various Co loadings. For the sake of comparison, the XRD patterns of $\text{P}/\gamma\text{-Al}_2\text{O}_3$ sample and single $\gamma\text{-Al}_2\text{O}_3$ supporter are also shown in Figure 1. In the case of the sample with higher Co loadings (CoP-10, CoP-20 and CoP-40), the XRD patterns showed diffraction peaks at 40.7, 42.1, 43.3, 44.1, 48.8, 50.4, 51.5, 52.0 and 56.2°, corresponding to the (112), (202), (211), (103), (031), (301), (113), (020) and (302) reflections of Co_2P (PDF-03-065-2380), respectively, except those diffraction peaks due to $\gamma\text{-Al}_2\text{O}_3$. The results indicated the formation of Co_2P on a $\gamma\text{-Al}_2\text{O}_3$ support. In the case of the sample with a lower Co loading (CoP-3), only diffraction peaks associated with the $\gamma\text{-Al}_2\text{O}_3$ support were apparent. This might be because Co-containing species was well dispersed on $\gamma\text{-Al}_2\text{O}_3$ supporter with higher surface area, as proved later by BET. It was worthy to note that there were several diffraction peaks at 20.5, 21.6 and 23.2° that can be assigned to orthorhombic AlPO_4 on

Table 1. Specific surface areas and CO chemisorption amounts of $\text{Co}_2\text{P}/\gamma\text{-Al}_2\text{O}_3$ catalysts obtained from the precursors with different Co loadings.

Sample	Co loading (wt%)	S_{BET} ($\text{m}^2 \text{g}^{-1}$)	CO chemisorption ($\mu\text{mol gcat}^{-1}$)
CoP-3	3	141.9	4.7
CoP-10	10	114.2	16.1
CoP-20	20	56.9	23.7
CoP-40	40	8.9	8.0

the CoP-40 sample. Due to the fact that the orthorhombic AlPO_4 phase can be formed on the P-20 sample via the reaction between P species and $\gamma\text{-Al}_2\text{O}_3$ (see Figure 1), it was reasonable to deduce that the orthorhombic AlPO_4 phase can be formed on the $\text{Co}_2\text{P}/\gamma\text{-Al}_2\text{O}_3$ catalysts. Interestingly, it was found from Figure 1 that the orthorhombic AlPO_4 phase can only be formed when the Co loading reached 40 wt%. This was probably because P species should be preferentially reacted with Co species to produce Co_2P and they had a chance to react with $\gamma\text{-Al}_2\text{O}_3$ to form AlPO_4 at higher P loadings.

The BET surface areas and CO chemisorption results of $\text{Co}_2\text{P}/\gamma\text{-Al}_2\text{O}_3$ catalysts obtained from the precursors with different Co loadings are listed in Table 1. The surface area of the catalysts decreased monotonically with the increase in Co loading, indicating that the Co_2P dispersity was decreased with the increase in Co loading. In addition, it was found that the CO chemisorption amount of the catalysts increased with the increase in Co loading from 3 to 20 wt%. However, the CO chemisorption amount of the catalyst decreased when the Co loading reached 40 wt%, which was probably due to the poor dispersion of CoP-40.

Subsequently, the morphologies of the catalysts were characterized by TEM. Figure 2 shows the TEM images of CoP-3, CoP-10, CoP-20 and CoP-40 samples. It was clear that irregular-shaped nanoparticles were dispersed on the $\gamma\text{-Al}_2\text{O}_3$ support. The size distributions of these nanoparticles in CoP-3, CoP-10, CoP-20 and CoP-40 samples were determined by measuring particle size directly from TEM images (Figure 3). It can be observed from Figure 3 that the average particle size of Co_2P varied with the Co loading. It was 25.3 nm in CoP-3, 36.7 nm in CoP-10, 46.9 nm in CoP-20 and 65.1 nm in CoP-40, respectively.

The PROX reactions under the conditions of twice excess O_2 (1%CO and 1% O_2 , 60% H_2 , He balance, 0.1 MPa, 15000 mL $\text{g}^{-1} \text{h}^{-1}$) were conducted on the $\text{Co}_2\text{P}/\gamma\text{-Al}_2\text{O}_3$ catalysts. The corresponding activity and selectivity measured at temperatures of 220 and 240 °C, are shown in Figure 4. Catalytic performance of the $\text{Co}_2\text{P}/\gamma\text{-Al}_2\text{O}_3$ catalysts for PROX was dependent on Co loading. It can be seen that Co-loading dependent CO conversion and CO_2 selectivity showed a “volcano” shape with the highest value (99.5% CO conversion at 220 °C and 98.5% CO conversion at 240 °C; 49.7% CO_2 selectivity at 220 °C and 48.0% CO_2 selectivity at 240 °C) on the CoP-10 sample. However, O_2 conversion was found to be 100% on these samples, no matter whether it was at 220 or 240 °C. The consumption of O_2 was much higher than that for CO oxidation, indicating an enhancement of H_2 oxidation in PROX. Generally speaking, specific surface area, the amount of active site and particle size were critical factors for the PROX catalyst.^[25–27] The ensemble of BET, TEM and CO chemisorption

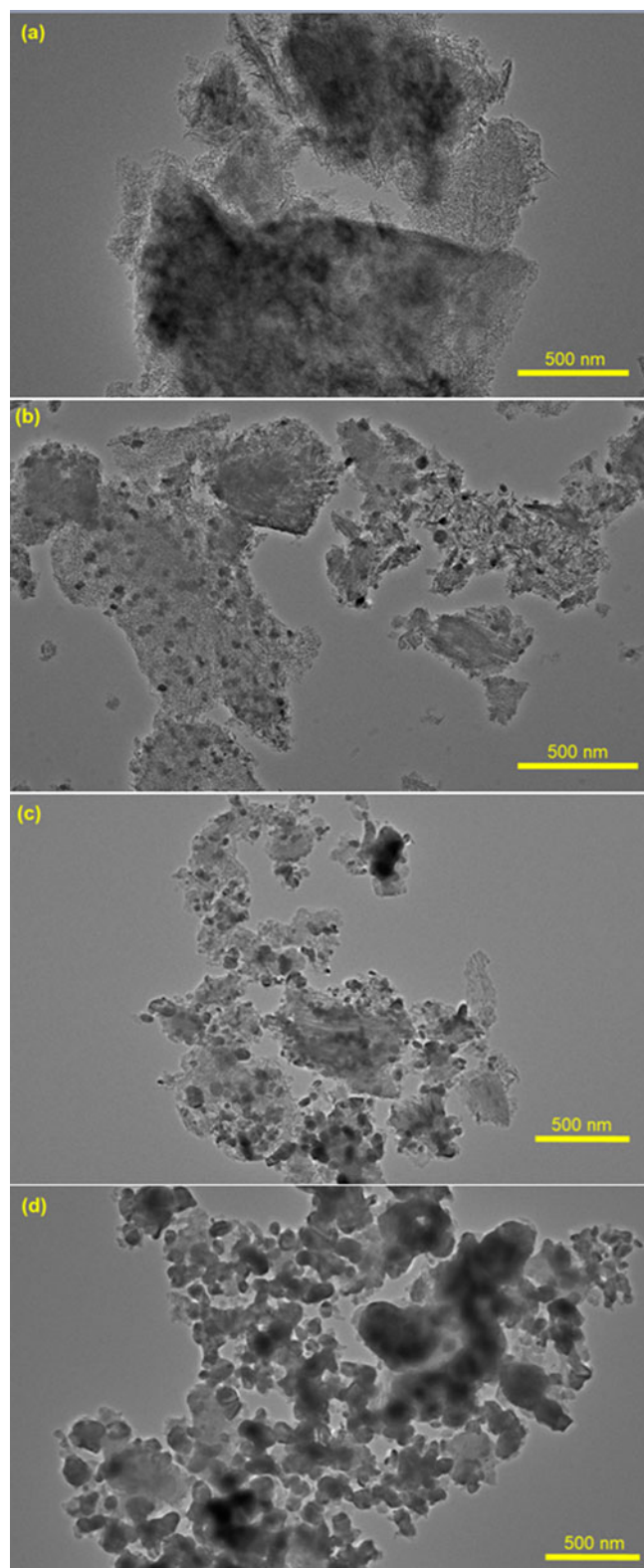


Figure 2. TEM images of (a) CoP-3, (b) CoP-10 (c) CoP-20 and (d) CoP-40 samples.

data (see Table 1 and Figures 2 and 3) indicated that among CoP-3, CoP-10, CoP-20 and CoP-40 samples, the CoP-10 sample showed the optimal microstructures (high surface area, small particle size and big amount of active site). Therefore, it was reasonable to conclude that the CoP-10 sample showed better PROX performance than CoP-3, CoP-20 and CoP-40

samples. In order to obtain a better evaluation of the $\text{Co}_2\text{P}/\gamma\text{-Al}_2\text{O}_3$ catalyst system, the CO conversion and CO_2 selectivity measured in the temperature range 160–240 °C are shown in Fig. S 1 (Supplemental Materials). And the CO conversion and CO_2 selectivity over the 2 wt%Pt/ $\gamma\text{-Al}_2\text{O}_3$ catalyst mentioned in our previous study^[28] is also shown for comparison. It was found that the CoP-10 sample showed higher CO conversion and CO_2 selectivity than CoP-3, CoP-20 and CoP-40 samples in the temperature range 160–240 °C. Note that the CoP-10 sample even showed similar PROX performance to 2 wt%Pt/ $\gamma\text{-Al}_2\text{O}_3$ catalyst in the temperature range 220–240 °C.

Finally, the time dependence of CO conversion and CO_2 selectivity at 220 °C over the CoP-10 sample is shown in Figure 5. Over the CoP-10 sample, the high CO conversion (~99.0%) was achieved and such activity was stable throughout the test period of 12 h.

Reaction conditions: 1% CO , 1% O_2 , 60% H_2 balanced with He, WHSV = 15,000 mL $\text{g}^{-1} \text{h}^{-1}$, reaction temperature = 220 °C, reaction time = 1–12 h, pressure = 0.1 MPa.

Experimental

Sample preparation

Alumina-supported Co_2P catalysts were prepared by the incipient wetness impregnation method. Firstly, the $\gamma\text{-Al}_2\text{O}_3$ supporter ($S_{\text{BET}} \approx 250 \text{ m}^2\text{g}^{-1}$, 40–60 mesh) was impregnated with an aqueous solution of $\text{Co}(\text{NO}_3)_2 \cdot 6\text{H}_2\text{O}$ and $(\text{NH}_4)_2\text{HPO}_4$ to give the desired Co/P molar ratio of 2 in the catalyst precursor. To avoid the formation of an insoluble precipitate of cobalt phosphate, several drops of nitric acid were introduced into the aqueous solution. After impregnation, the samples were dried in air at 100 °C for 12 h and then calcined in air at 500 °C for 3 h. The $\text{Co}_2\text{P}/\gamma\text{-Al}_2\text{O}_3$ samples were prepared by means of H_2 -temperature-programmed reaction ($\text{H}_2\text{-TPR}$).^[12,13] Typically, about 2.0 g of the precursor was placed in a micro-reactor and a flow of H_2 (150 ml min^{-1}) was introduced into the system. Initially, the sample was linearly heated from room temperature (RT) to 300 °C over a period of 30 min, followed by a rise in temperature from 300 to 700 °C at a rate of 1 °C/min, and the temperature was then kept at 700 °C for 2 h before cooling to RT in a H_2 flow. The material was then passivated in 1% $\text{O}_2/99\%$ Ar for 12 h before exposure to air. The catalyst precursors contained Co loadings of 3, 10, 20, 40 wt% and the as-obtained phosphide catalysts were designated respectively as CoP-3, CoP-10, CoP-20 and CoP-40. For the sake of comparison, the catalyst only with 20 wt% P (designated as P-20) was also obtained and the preparation procedures were similar to those $\text{Co}_2\text{P}/\gamma\text{-Al}_2\text{O}_3$ catalysts.

Sample characterizations

X-ray diffraction (XRD) measurements were carried out using Cu $K\alpha$ source with a X'Pert Pro MPD diffractometer. The morphology of the product was characterized by transmission electron microscopy (TEM, Philips Tecna 10). BET surface areas of the products were measured by a surface

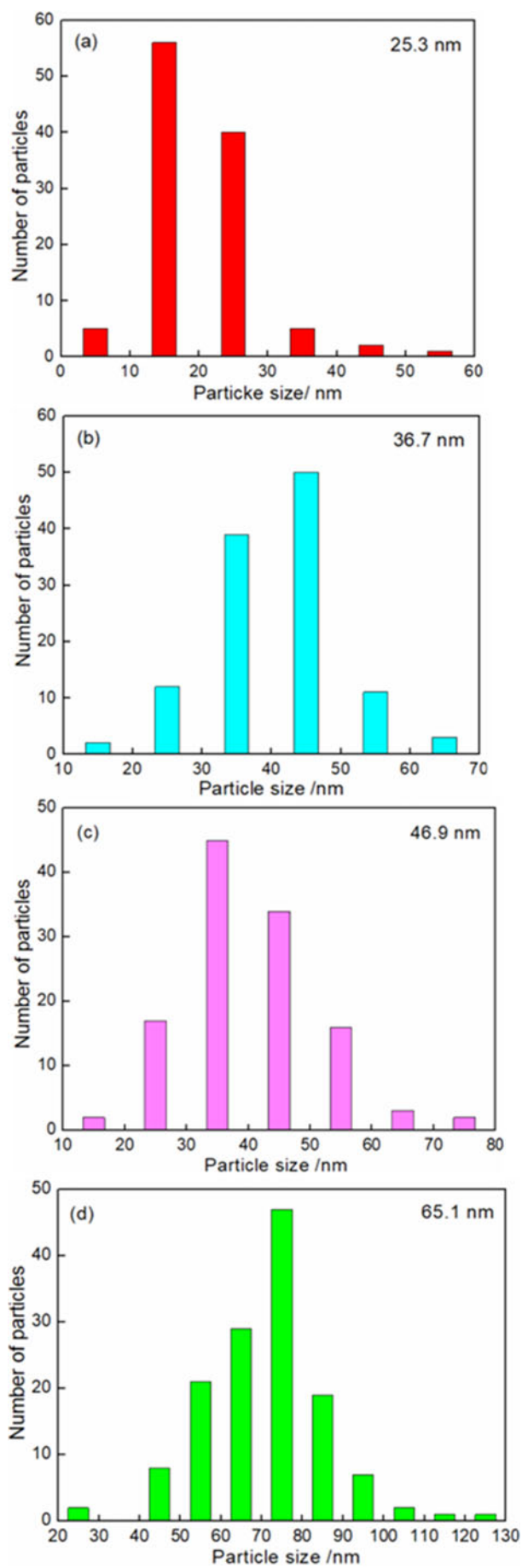


Figure 3. Particle size distributions of Co_2P nanoparticles in (a) CoP-3, (b) CoP-10 (c) CoP-20 and (d) CoP-40 samples.

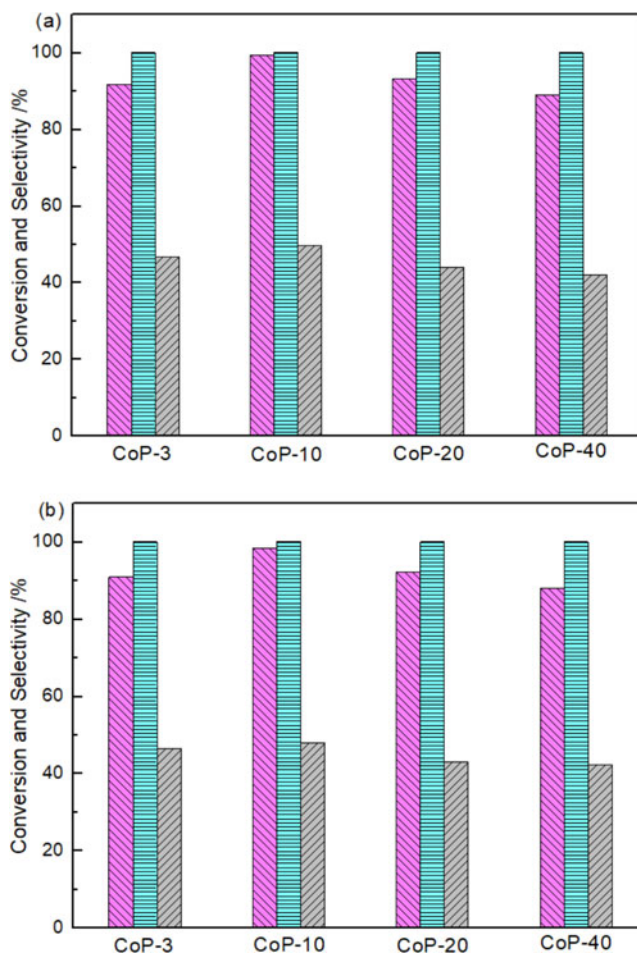


Figure 4. Dependence of catalytic performance on Co loading over the $\text{Co}_2\text{P}/\gamma\text{-Al}_2\text{O}_3$ catalysts at 220 °C (a) and 240 °C (b). (▨) CO conversion, (■) O_2 conversion and (▩) CO_2 selectivity. Reaction conditions: 1% CO , 1% O_2 , 60% H_2 balanced with He, WHSV = 15,000 $\text{mL g}^{-1} \text{h}^{-1}$, reaction temperature = 220–240 °C, pressure = 0.1 MPa.

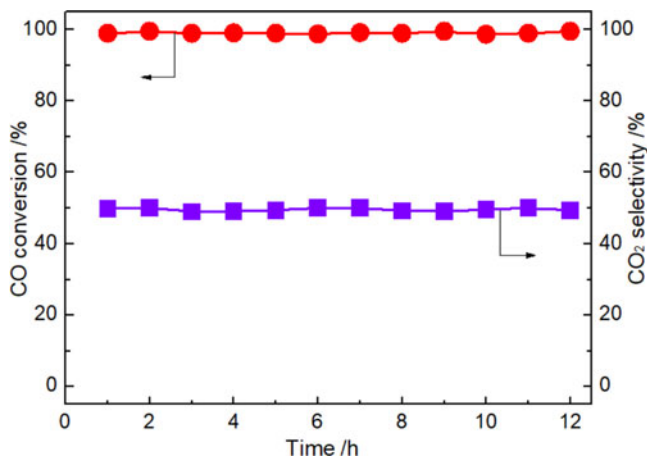


Figure 5. Catalytic stability of the CoP-10 catalyst in PROX reaction.

area analyzer (NOVA4200). CO chemisorption experiments were carried out in an AutoChem II chemisorption Analyzer. 0.1 g catalyst was firstly reduced in a flow of 10% H_2/Ar at 700 °C for 1 h. After purging with He for 30 min, the sample was cooled down to 30 °C in He. The adsorption of CO was carried out by pulsing a standard

volume of pure CO until saturation. CO consumption was detected by a thermal conductivity detector (TCD).

Catalytic performance tests

PROX reaction was carried out in a fixed-bed flow reaction system at atmospheric pressure. The catalyst was placed in a quartz reactor (id: 4 mm) equipped with devices for temperature measurement and control. The feed gas consisted of 50 ml min⁻¹ of 1%CO, 1%O₂, 60%H₂ in He (WHSV = 15,000 ml g⁻¹ h⁻¹). Before each test, the catalyst was heated to 700 °C at a rate of 15 °C/min and was held at this temperature for 1 h in a flow of H₂. The effluent gas was analyzed using on-line gas chromatograph (GC) system equipped with a TCD detector. The activity was evaluated based on CO and O₂ conversions, which can be calculated on the basis of CO and O₂ concentrations in the reactant gas and the effluent gas. Due to possibility of CH₄ produced in PROX reaction, the CO₂ selectivity was defined as the ratio of O₂ consumption for the CO oxidation to total O₂ consumption.

Conclusions

We developed a novel type of alumina-supported Co₂P catalyst for PROX reaction. It was found that the catalytic activities of these Co₂P/γ-Al₂O₃ catalysts were related to their Co loadings. The Co₂P/γ-Al₂O₃ catalyst prepared from the precursor with 3 wt% Co loading showed the best PROX activity (near 99% CO conversion) in temperature range of 220–240 °C, which was attributed to its optimal microstructures (high surface area, small particle size and big amount of active site).

Disclosure statement

No potential conflict of interest was reported by the authors.

Funding

The work was supported by the National Natural Science Foundation of China (No. 21276253), the Project of Liaoning Province Department of Education (No. L2017LZD003) and the Natural Science Foundation of Liaoning Province (No. 20180551272).

ORCID

Zhiwei Yao  <http://orcid.org/0000-0002-2535-9808>

Qingyou Liu  <http://orcid.org/0000-0002-5630-7680>

References

- Yoon, K. Y.; Jang, Y.; Park, J.; Hwang, Y.; Koo, B.; Park, J.-G.; Hyeon, T. Synthesis of Uniform-sized Bimetallic Iron-nickel Phosphide Nanorods. *J. Solid State Chem.* **2008**, *181*, 1609–1613. DOI: [10.1016/j.jssc.2008.05.022](https://doi.org/10.1016/j.jssc.2008.05.022).
- Popczun, E. J.; McKone, J. R.; Read, C. G.; Biacchi, A. J.; Wiltrout, A. M.; Lewis, N. S.; Schaak, R. E. Nano Structured Nickel Phosphide as an Electro Catalyst for the Hydrogen Evolution Reaction. *J. Am. Chem. Soc.* **2013**, *135*, 9267–9270. DOI: [10.1021/ja403440e](https://doi.org/10.1021/ja403440e).
- Jiang, X. C.; Xiong, Q. H.; Nam, S.; Qian, F.; Li, Y.; Lieber, C. M. InAs/InP Radial Nanowire Heterostructures as High Electron Mobility Devices. *Nano Lett.* **2007**, *7*, 3214–3218. DOI: [10.1021/nl072024a](https://doi.org/10.1021/nl072024a).
- Alexander, A.-M.; Hargreaves, J. S. J. Alternative Catalytic Materials: Carbides, Nitrides, Phosphides and Amorphous Boron Alloys. *Chem. Soc. Rev.* **2010**, *39*, 4388–4410. DOI: [10.1039/b916787k](https://doi.org/10.1039/b916787k).
- Abu, I. I.; Smith, K. J. The Effect of Cobalt Addition to Bulk MoP and Ni₂P Catalysts for the Hydrodesulfurization of 4,6-Dimethyldibenzothiophene. *J. Catal.* **2006**, *241*, 356–366. DOI: [10.1016/j.jcat.2006.05.010](https://doi.org/10.1016/j.jcat.2006.05.010).
- Wang, X.; Clark, P.; Oyama, S. T. Synthesis, Characterization, and Hydrotreating Activity of Several Iron Group Transition Metal Phosphides. *J. Catal.* **2002**, *208*, 321–331. DOI: [10.1006/jcat.2002.3604](https://doi.org/10.1006/jcat.2002.3604).
- Ding, L.; Shu, Y.; Wang, A.; Zheng, M.; Li, L.; Wang, X.; Zhang, T. Preparation and Catalytic Performances of Ternary Phosphides NiCoP for Hydrazine Decomposition. *Appl. Catal. A.* **2010**, *385*, 232–237. DOI: [10.1016/j.apcata.2010.07.020](https://doi.org/10.1016/j.apcata.2010.07.020).
- Cheng, R.; Shu, Y.; Zheng, M.; Li, L.; Sun, J.; Wang, X.; Zhang, T. Molybdenum Phosphide, a New Hydrazine Decomposition Catalyst: Microcalorimetry and FTIR Studies. *J. Catal.* **2007**, *249*, 397–400. DOI: [10.1016/j.jcat.2007.04.007](https://doi.org/10.1016/j.jcat.2007.04.007).
- Zheng, M.; Shu, Y.; Sun, J.; Zhang, T. Carbon-covered Alumina: A Superior Support of Noble Metal-like Catalysts for Hydrazine Decomposition. *Catal. Lett.* **2008**, *121*, 90–96. DOI: [10.1007/s10562-007-9300-9](https://doi.org/10.1007/s10562-007-9300-9).
- Feng, L.; Vrabel, H.; Bensimon, M.; Hu, X. Easily-prepared Dinickel Phosphide (Ni₂P) Nanoparticles as an Efficient and Robust Electrocatalyst for Hydrogen Evolution. *Phys. Chem. Chem. Phys.* **2014**, *16*, 5917–5921. DOI: [10.1039/c4cp00482e](https://doi.org/10.1039/c4cp00482e).
- Popczun, E. J.; Read, C. G.; Roske, C. W.; Lewis, N. S.; Schaak, R. E. Highly Active Electrocatalysis of the Hydrogen Evolution Reaction by Cobalt Phosphide Nanoparticles. *Angew. Chem.* **2014**, *126*, 5531–5534. DOI: [10.1002/ange.201402646](https://doi.org/10.1002/ange.201402646).
- Yao, Z.; Dong, H.; Shang, Y. Catalytic Activities of Iron Phosphide for NO Dissociation and Reduction with Hydrogen. *J. Alloys Compd.* **2009**, *474*, L10–L13. DOI: [10.1016/j.jallcom.2008.06.072](https://doi.org/10.1016/j.jallcom.2008.06.072).
- Yao, Z.; Qiao, X.; Liu, D.; Shi, Y.; Zhao, Y. Catalytic Activities of Transition Metal Phosphides for NO Dissociation and Reduction with CO. *Chem. Biochem. Eng. Q.* **2016**, *29*, 505–510. DOI: [10.15255/CABEQ.2014.2133](https://doi.org/10.15255/CABEQ.2014.2133).
- Xu, H.; Fu, Q.; Yao, Y.; Bao, X. Highly Active Pt-Fe Bicomponent Catalysts for CO Oxidation in the Presence and Absence of H₂. *Energy Environ. Sci.* **2012**, *5*, 6313–6320. DOI: [10.1039/C1EE02393D](https://doi.org/10.1039/C1EE02393D).
- Qiao, B.; Wang, A.; Li, L.; Lin, Q.; Wei, H.; Liu, J.; Zhang, T. Ferric Oxide-supported Pt Subnano Clusters for Preferential Oxidation of CO in H₂-rich Gas at Room Temperature. *ACS Catal.* **2014**, *4*, 2113–2117. DOI: [10.1021/cs500501u](https://doi.org/10.1021/cs500501u).
- Mu, R.; Fu, Q.; Xu, H.; Zhang, H.; Huang, Y.; Jiang, Z.; Zhang, S.; Tan, D.; Bao, X. Synergetic Effect of Surface and Subsurface Ni Species at Pt-Ni Bimetallic Catalysts for CO Oxidation. *J. Am. Chem. Soc.* **2011**, *133*, 1978–1986. DOI: [10.1021/ja109483a](https://doi.org/10.1021/ja109483a).
- Pan, Y.; Hwang, S. Y.; Shen, X.; Yang, J.; Zeng, J.; Wu, M.; Peng, Z. Computation-Guided Development of Platinum Alloy Catalyst for Carbon Monoxide Preferential Oxidation. *ACS Catal.* **2018**, *8*, 5777–5786. DOI: [10.1021/acscatal.8b00154](https://doi.org/10.1021/acscatal.8b00154).
- Ko, E.-Y.; Park, E. D.; Lee, H. C.; Lee, D.; Kim, S. Supported Pt-Co Catalysts for Selective CO Oxidation in a Hydrogen-rich Stream. *Angew. Chem. Int. Ed. Engl.* **2007**, *46*, 734–737. DOI: [10.1002/anie.200603144](https://doi.org/10.1002/anie.200603144).
- Gamarra, D.; Belver, C.; Fernandez-García, M.; Martínez-Arias, A. Selective CO Oxidation in Excess H₂ Over Copper-ceria Catalysts: Identification of Active Entities/Species. *J. Am. Chem. Soc.* **2007**, *129*, 12064–12065. DOI: [10.1021/ja073926g](https://doi.org/10.1021/ja073926g).

- [20] Hornés, A.; Hungría, A. B.; Bera, P.; Cámara, A. L.; Fernández-García, M.; Martínez-Arias, A.; Barrio, L.; Estrella, M.; Zhou, G.; Fonseca, J. J.; Inverse CeO₂/CuO Catalyst as an Alternative to Classical Direct Configurations for Preferential Oxidation of CO in Hydrogen-rich Stream. *J. Am. Chem. Soc.* **2010**, *132*, 34–35. DOI: [10.1021/ja9089846](https://doi.org/10.1021/ja9089846).
- [21] Davó-Quiñonero, A.; Navlani-García, M.; Lozano-Castelló, D.; Bueno-López, A.; Anderson, J. A. Role of Hydroxyl Groups in the Preferential Oxidation of CO over Copper Oxide-Cerium Oxide Catalysts. *ACS Catal.* **2016**, *6*, 1723–1731. DOI: [10.1021/acscatal.5b02741](https://doi.org/10.1021/acscatal.5b02741).
- [22] Lin, J.; Qiao, B.; Liu, J.; Huang, Y.; Wang, A.; Li, L.; Zhang, W.; Allard, F.; Wang, X.; Zhang, T. Design of a Highly Active Ir/Fe(OH)_x Catalyst: Versatile Application of Pt-group Metals for the Preferential Oxidation of Carbon Monoxide. *Angew. Chem. Int. Ed.* **2012**, *51*, 2920–2924. DOI: [10.1002/anie.201106702](https://doi.org/10.1002/anie.201106702).
- [23] Qiao, B.; Liu, J.; Wang, Y. G.; Lin, Q.; Liu, X.; Wang, A.; Li, J.; Zhang, T.; Liu, J. Highly Efficient Catalysis of Preferential Oxidation of CO in H₂-rich Stream by Gold Single-atom Catalysts. *ACS Catal.* **2015**, *5*, 6249–6254. DOI: [10.1021/acscatal.5b01114](https://doi.org/10.1021/acscatal.5b01114).
- [24] Yeung, C. M. Y.; Tsang, S. C. Some Optimization in Preparing Core-shell Pt–ceria Catalysts for Water Gas Shift Reaction. *J. Mol. Catal. A* **2010**, *322*, 17–25. DOI: [10.1016/j.molcata.2010.02.001](https://doi.org/10.1016/j.molcata.2010.02.001).
- [25] Xu, J.; Xu, X.; Ouyang, L.; Yang, X.; Mao, W.; Su, J.; Han, Y. Mechanistic Study of Preferential CO Oxidation on a Pt/NaY Zeolite Catalyst. *J. Catal.* **2012**, *287*, 114–123. DOI: [10.1016/j.jcat.2011.12.012](https://doi.org/10.1016/j.jcat.2011.12.012).
- [26] Kim, Y. H.; Park, E. D. The Effect of the Crystalline Phase of Alumina on the Selective CO Oxidation in a Hydrogen-rich Stream over Ru/Al₂O₃. *Appl. Catal. B.* **2010**, *96*, 41–50. DOI: [10.1016/j.apcatb.2010.02.001](https://doi.org/10.1016/j.apcatb.2010.02.001).
- [27] Yao, Z.; Zhang, X.; Peng, F.; Yu, H.; Wang, H.; Yang, J. Novel Highly Efficient Alumina-supported Cobalt Nitride Catalyst for Preferential CO Oxidation at High Temperatures. *Int. J. Hydrogen Energy.* **2011**, *36*, 1955–1959. DOI: [10.1016/j.ijhydene.2010.11.082](https://doi.org/10.1016/j.ijhydene.2010.11.082).
- [28] Chang, X.; Shi, Y.; Yao, Z.; Kang, X.; Jiang, B.; Sun, Y. Novel Cobalt Nitride-induced Oxygen Activation on Pt-based Catalyst for Catalytic Oxidation. *Phosphorus Sulfur Silicon Relat. Elem.* DOI: [10.1080/10426507.2018.1513935](https://doi.org/10.1080/10426507.2018.1513935).